University Library

MINERVA ACCESS

A gateway to Melbourne's research publications

Minerva Access is the Institutional Repository of The University of Melbourne

Author/s:
Li, J;Hutchison, JA;Smith, D;Wu, H;Mulvaney, P

Title:
Ultrafast Nanodrum-on-Chip Pixels

Date:
2024-04-17

Citation:
Li, J., Hutchison, J. A., Smith, D., Wu, H. & Mulvaney, P. (2024). Ultrafast Nanodrum-on-Chip Pixels. Nano Letters, 24 (15), pp.4362-4368. https://doi.org/10.1021/acs.nanolett.3c04840.

Persistent Link:
https://hdl.handle.net/11343/345166

Ultrafast Nanodrum-on-Chip Pixels

Jialu Li,[†] James Hutchison,[†] Dan Smith,[‡] Hao Wu,[¶] and Paul Mulvaney[*,†]

†*ARC Centre of Excellence in Exciton Science, School of Chemistry, the University of Melbourne, Parkville, VIC., 3010, Australia*

‡*Melbourne Centre for Nanofabrication, 151 Wellington Road Clayton, VIC., 3168, Australia.*

¶*Chinese Academy of Sciences Chongqing Green Intelligence Technology, Beibei, Chongqing, 400713, China*

E-mail: mulvaney@unimelb.edu.au

Abstract

Environmentally friendly, ultrafast display pixels of micron sizes are fabricated with nanometre-thick gold films and Si/SiO_2 wafers. The colour displayed is due to both the plasmon response of the gold film and the optical interference from the Fabry–Pérot cavity formed by the underlying silicon substrate, the semi-transparent gold film and the air gap between them. When an electric potential is applied to the gold film, the electrostatic force induces attraction between the gold film and the silicon wafer. Due to the flexibility of the film, the size of the air gap changes, resulting in a changing colour. By applying different driving signals, we have achieved cyan, magenta and yellow reflected colours. The maximum switching rate of the pixel is primarily determined by the thickness dependence of the metal drum and the Young's modulus and is typically in the MHz regime.

Keywords: Gold, Fabry-Pérot, Reflective Display, Resonator

Introduction

E-ink displays are paper-like and can work under natural light without glare. As a result, they induce less fatigue and visual strain, and are therefore easier to read compared to light emitting displays based on LCD or OLED platforms.[1,2] However, current E-ink readers use the movement of black and white particles in fluids to render images, and these are slow in terms of refresh rate, are prone to leaks and colour images are difficult to realise.[3,4] As a result, an easy-to-view colour display strategy reaching high refresh rate remains desirable. One approach to realise reflective display with various colours is to use tunable Fabry-Pérot (FP) cavities to modulate light.[5,6] Ultrathin metal films can act as the top layer, having both the elastic properties needed for stable switching as well as thickness dependent light transmission.[7–11] Due to the selectivity of an FP cavity, one can achieve high light absorption or reflectivity over a narrow bandwidth by engineering the refractive index of the dielectric material and the thickness of the cavity.[7,12,13] For example, metasurfaces have been introduced in order to modulate the refractive index. However, such structures lack real-time spectral tunability.[14] Hydrogels whose refractive index and length alters according to the humidity of the environment allow colour changes to occur in response to hydrogel swelling. However, the time scale for the colour change is about 10 minutes due to the slow response of the hydrogel to humidity.[15] Interferometric modulator displays (IMOD) employ deformable membranes and can reach a switching time of tens of microseconds. But the display pixel itself consists of 3 single-colour (red, green, blue) subpixels, making the device structure extremely complicated.[16] Pixels using the electromechanical deformation of graphene films have also been reported, with a narrow colour tuning range due to the high transparency of graphene.[17]

Here we propose an ultrafast,[18–20] interferometric, tunable display pixel in the form of a metal nanodrum based FP cavity. The drum uses a thin gold film as the semi-transparent mirror and silicon as the reflective mirror. By tailoring the cavity thickness, cyan is displayed in the neutral state. The film is deformable, leading to a thickness change of the FP cavity,

and hence colour change. The pixel can operate under both DC and AC driving signals. Due to the flexibility of the film, the frame rate can reach megahertz frequencies. As will be shown, the colour gamut can be widened by creating a small hole in the film which reduces the interfacial tension. Cyan, magenta and yellow colours can be achieved by tuning both the top and back voltages. A spectral shift of 100 nm can be realised within an 8-volt driving range. We believe such low power-consumption ultrafast display pixels can create a pathway for electronic papers and video recording applications.

Results and Discussion

Figure 1 (a) shows a schematic of the nanodrum pixel. The pixel consists of a nanometre thick gold film and a patterned SiO_2/silicon substrate. The lossy gold film acts as a semi-transparent mirror and the underlying opaque silicon acts as the reflective mirror. The film and the silicon comprise a FP cavity with air as the intermediate dielectric layer. The patterned SiO_2 layer provides mechanical support and dielectric isolation for the gold film.[21] When white light is incident on the drum pixel, a certain wavelength is resonant with the cavity and thus absorbed. The complementary colour of the resonance wavelength will be displayed. Since this colour effect is subtractive, the CMY colour scheme is more applicable than the RGB scheme to evaluate it.[22] When a voltage is applied between the gold film and the silicon, it induces an electrostatic force between the film and the silicon substrate, causing the gold thin film to deform towards the silicon.[23–25] When the electrostatic force is in equilibrium with the elastic restoring force due to the film deformation, a steady state is reached.

The applied voltage results in a decrease in the cavity thickness and thus the absorbed colour shifts to shorter wavelengths. The wavelength that is absorbed by the cavity corresponds to the minimum in the reflection spectrum. As cyan is the complement of red, magenta is the complement of green and yellow is the complement of blue, in order to reach

these three essential colours, the colour displayed at the neutral state ($V_{\mathrm{T}} = V_{\mathrm{B}} = 0$) should be cyan, as it requires the thickest cavity. Figure 1 (b) shows an optical microscope image of the pixel in the neutral state; the drum evinces a uniform cyan colour. Figure 1 (c) shows a cross-section of an empty circular well with a diameter of 10 µm and with the gold thin film suspended over it. The corresponding AFM profiles are shown in Figure S1, showing a cavity depth of about 271 nm. The COMSOL simulation in Figure 1 (d) indicates the cavity depth should be around 270 nm in order to display a cyan colour. The reflection spectrum taken at the centre of the pixel shows good agreement with the simulation results.

Since the steady state deflection of the film depends on the elastic restoring force, the colour range tuned within the same voltage range should be dependent on the drum diameter. In fact, it can be seen from the AFM results shown in Figure S2 that the droop of drums of different sizes is almost constant, indicating similar cavity thicknesses. This is also evident from the consistent colours displayed by the pixels of different sizes, shown in Figure S3.

We now apply a DC bias to the gold drums. The reflection spectra collected at the centres of the pixels of different sizes for different values of V_{T} are shown in Figure S4 and optical microscope images of the pixels of different diameters when the top voltage is 5 V are shown in Figure S5. We plot the wavelengths corresponding to the minima of the spectra, which are the absorption peaks, as a function of the top voltage in Figure 1 (e). As the voltage increases, the minima all blue-shift and the magnitude of the shift increases with increasing drum diameter. This is more obvious when we plot the shift as a function of diameter as shown in Figure 1 (f). This means that a larger diameter is beneficial for a wider colour gamut.

To understand the deformation induced by the applied voltages, we have investigated the role of V_{T} and V_{B} separately. An unusual asymmetry is observed. Figure 2 shows the single-voltage induced spectral shifts of the 10 µm drum in Figure 1 (c). To study the effect of the top voltage, we first ground the back electrode and apply different DC biases to the gold film. The DC voltage changes from -5 V to 5 V with a step of 1 V. As the thickness of

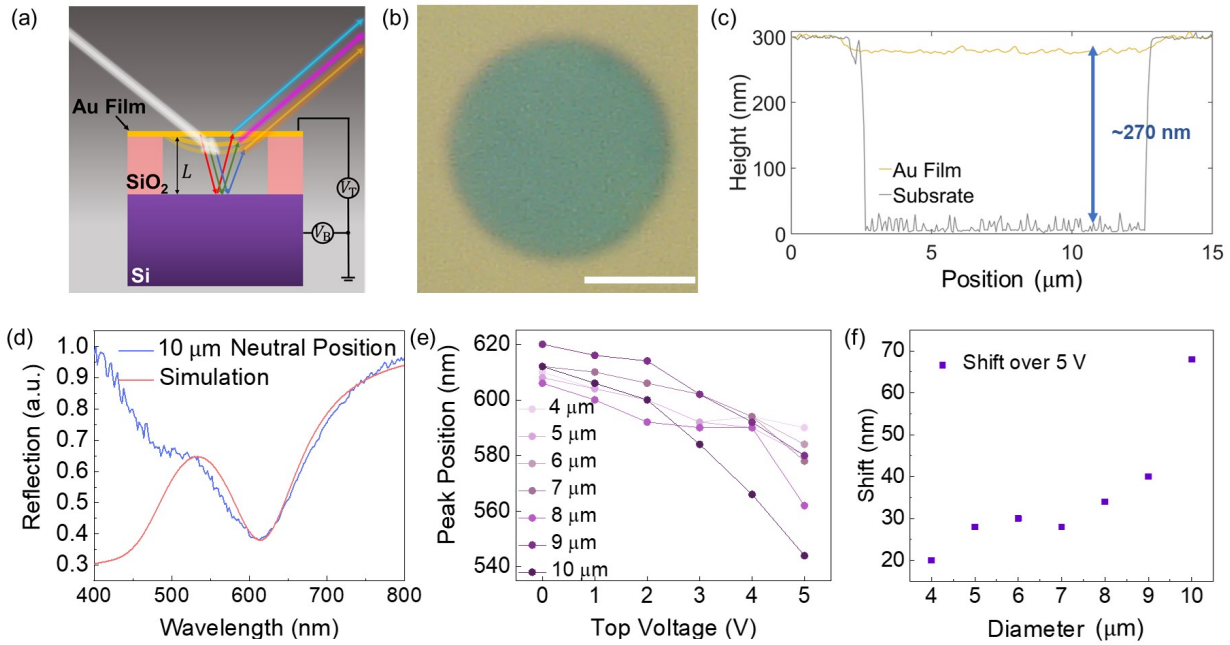


Figure 1: **Schematic and size dependence of the colour of the pixels.** (a) Schematic of the colour display and control of the nanodrum-on-chip pixel. V_{T} stands for the top voltage, which is applied to the gold thin film. V_{B} stands for the back voltage, which is applied to the underlying silicon. (b) Optical microscope image of a circular pixel with a diameter of 10 microns in its neutral state. The thickness of the gold film is 28 nm. (c) AFM profiles of a thin gold film suspended over an empty cavity and the topography of the empty cavity. The drum is circular with a diameter of 10 microns. The distance between the film and the bottom silicon substrate is around 270 nm. (d) Reflection spectrum of the drum shown in (c) in its natural position. The solid line is the experimental data and the dotted line is the prediction from simulations using Comsol Multiphysics. (e) The wavelength of the minima in the reflection spectra for drums of different diameters as a function of the applied drum voltage. (f) Spectral shift as a function of the drum diameter for a fixed top voltage of 5 V.

the gold film is on the nanometre scale, the melting point of the gold drum is significantly lower than that of the bulk metal.[26] At a voltage higher than 5 V, the heat generated by the transient current can cause melting of the drumhead and hence we limited the applied voltage to 5V.

Optical microscope images of the 10 µm drum as a function of the top voltage are shown in Figure S6. It can be seen that the deformation of the film increases as the voltage increases. The reflection spectra taken at the centre of the drum for different voltages are plotted in Figure 2 (a). For clear visualisation, only the spectra at 0 V, ± 3 V and ± 5 V are presented. As the amplitude of the bias increases, the minima in the spectra undergo a blue shift, indicating the electrostatic forces between the top gold film and the underlying silicon are increasing. However, negative bias can induce slightly larger shifts in comparison to a positive bias of the same amplitude. The trend is more obvious when we plot the spectral intensity contours as a function of the applied voltage, as shown in Figure 2 (b). The scales of the colour bar correspond to the reflection intensities and the darkest colour corresponds to the absorption peak. The spectra are relatively symmetric with respect to 0 V with a slightly larger change on the negative side. At 1 volt, the difference between positive and negative biases is about 2 nm, however it increases to 16 nm at 5 volts, as shown in Figure 2 (c). The experimental results for the same drum pixel at $V_{\mathrm{T}} = 5$ V and the corresponding simulations are shown in Figure S7. We can see that a 5 V top voltage corresponds to a cavity thickness of 225 nm, equivalent to a deflection of 35 nm from the neutral state. Under -5 V, the deflection increases to 214 nm. Such asymmetry is probably due to the fact that the bottom n-type silicon electrode is a semiconductor. Unlike gold, which is instantly polarized when a voltage is applied, it takes time for electrons and holes to reach equilibrium under the applied electric field. As we used n-type silicon, the mobility of electrons is higher than that of the holes and the electron concentration is at least a factor of 10^6 higher than the hole concentration. When a positive top voltage (negative bottom voltage) is applied, the electrons move toward the gold film until the electrostatic force balances the tensile forces

acting on the gold film. When a negative top voltage (positive bottom voltage) is applied, there is a much smaller concentration of holes moving towards the gold film (and a high concentration of more mobile electrons moving away from the surface), which results in a longer drum deformation time. In the next step, we ground the top electrode and change the back voltage applied to the silicon. The back voltage is a DC bias changing from -10 V to 10 V. The absorption peak wavelength is plotted in Figure 2 (d) as a function of back voltage. Though applied back voltages induce less damage to the gold films compared to top voltages, it is obvious that the back voltage induces smaller spectral shifts. For a 10-volt bias, only 60 nm shifts can be induced. For back voltage modulation, the spectral asymmetry is again observed. For the same amplitude, positive back voltage induces larger spectral shifts compared to negative voltage, which is consistent with the top voltage pattern, validating our assumption. The corresponding reflection spectra and the spectrum contour are shown in Figure S8.

A wider colour range can be achieved by the judicious combination of applied top and back voltages with opposite polarities. Figure 3 (a) shows the reflection spectra taken from the centre of the 10 µm drum when the top voltage is 5 V and the back voltage changes from 0 V to -2 V. Figure 3 (b) shows the counterparts when the top voltage is -5 V and the back voltage changes from 0 V to 2 V. It is obvious that a combination of top and back voltages of opposite polarity can blue-shift the spectra further. As mentioned above, negative top voltages and positive back voltages create larger shifts by themselves. Such differences are more obvious when the top and back voltage are applied simultaneously. We plot the wavelength of the reflection spectrum minima corresponding to the back voltage in Figure 3 (c). It is evident that a negative top voltage plus a positive back voltage induces a larger wavelength change than the opposite combination.

In experiments, the damage threshold for a pixel with a diameter of 10 microns is 7 volts ($V_{\mathrm{T}} = -5$ V, $V_{\mathrm{B}} = 2$ V).

The pixel shows excellent high frequency AC performance, which is discussed in detail

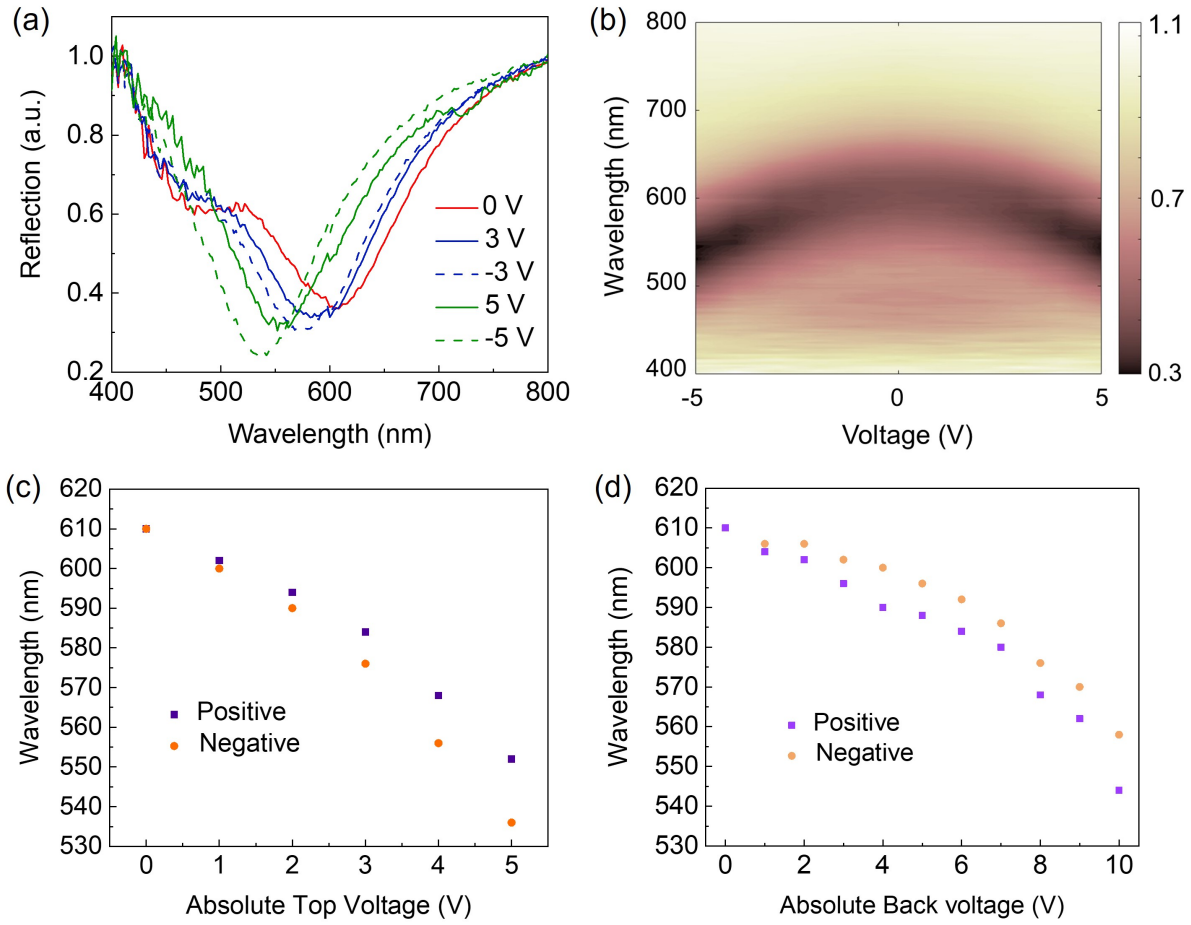


Figure 2: **Spectral shifts induced by top voltage and back voltage** (a) Reflection spectra taken in the centre of the drum in Fig.1 (c) when the top voltage changes from -5 V to 5 V. The back electrode is kept grounded. (b) Reflection spectra as a function of top voltage. (c) Wavelength of the spectral minima of the drum as a function of the applied top voltage. (d) Wavelength of the spectral minima of the drum as a function of the applied back voltage.

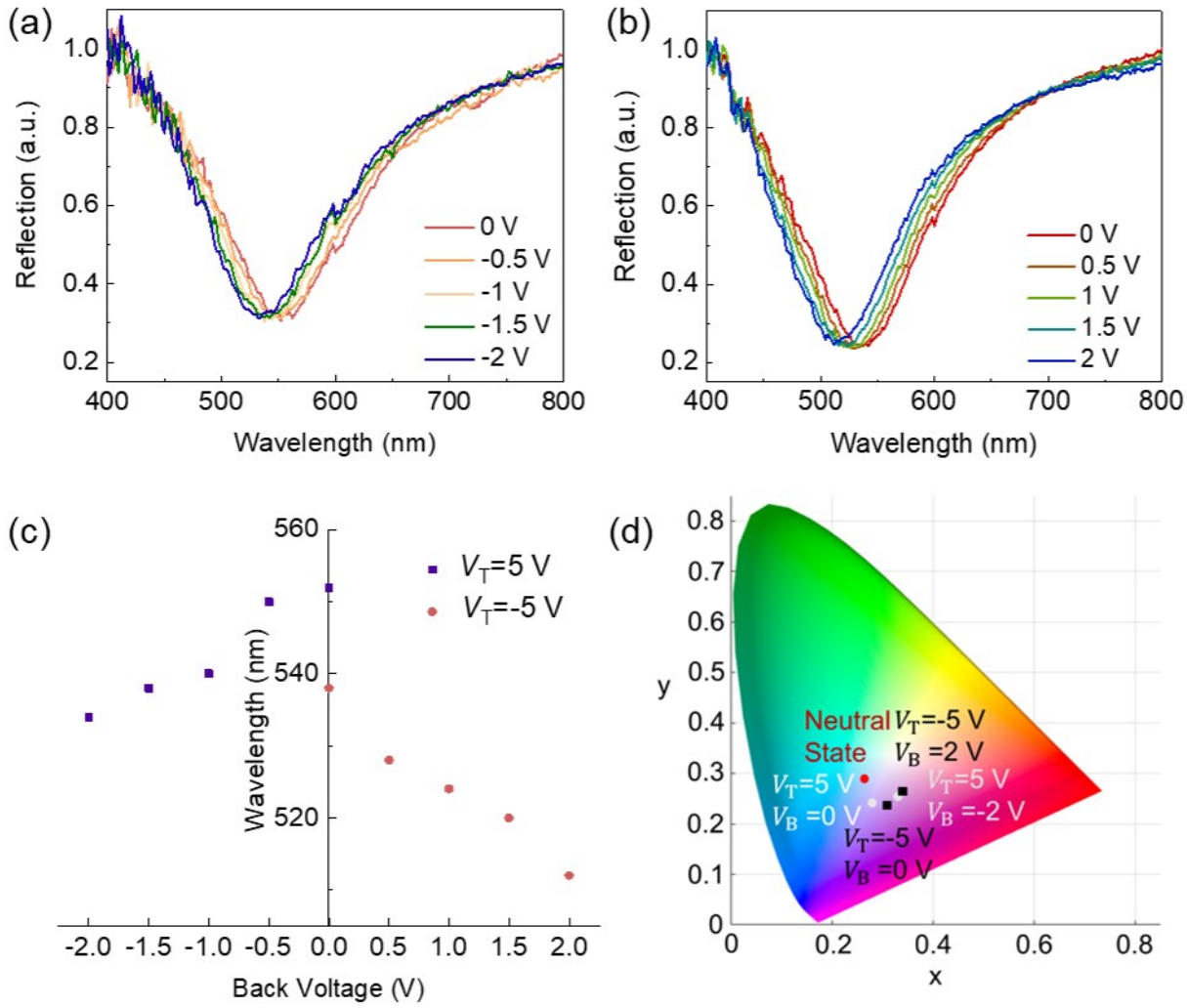


Figure 3: **Synergistic effects of top voltage and back voltage.** Reflection spectra taken at the centre of the drum in Fig.1 (c) (a) when the top voltage is 5 V and the back voltage changes from 0 V to -2 V and (b) when the top voltage is -5 V and back voltage changes from 0 V to 2 V. (c) Wavelengths of the spectral minima of the drum corresponding to different voltage combinations. (d) CIE colour coordinates of the colour displayed at several voltage combinations.

in Section 2 of the Supporting Information. It can be seen that in kHz regime, the pixel shows excellent colour response. In MHz regime, there might be some interaction between the electronic signal and the natural vibration frequencies of the drum.[21] Nevertheless, the pixel can response as a frequency up to MHz. Such high refresh speeds open up potential applications in information storage technologies and fast electro-optical switching.

As mentioned before, in DC mode, we keep the absolute voltage difference between the top and bottom electrodes within 7 volts. Above that value, the film rigidity and the built-in tension cannot counterbalance the electric field and the drum ruptures. To address this limitation, we create a small hole in the centre of the drum and release the in-built tension. Figure 4 (a) shows the reflection spectra taken at the centre of the gold drum as a function of voltage before (I) and after (D) a minor defect is created. As the devices were fabricated in air, it is inevitable that air was trapped in the cavity. It has been reported that the hydrostatic force induced by the gas pressure inside may affect the mechanical behaviour of thin films.[17] For our device, the reflection spectra are almost identical in both cases. This indicates that the hydrostatic forces caused by the increased gas pressure inside the drum are negligible in our case. For these perforated drums, we can apply a voltage difference of 8 V, i.e., $V_{\mathrm{T}} = -5\mathrm{V}$ and $V_{\mathrm{T}} = 3\mathrm{V}$. The minimum in the reflection spectrum further blue-shifts, and the deflection can now exceed 100 nm relative to the neutral state. Figure 4 (b) shows hyperspectral images taken at 600 nm of the perforated drum when different voltages are applied, and the corresponding optical microscope images are shown in Figure 4 (c). (i) is the neutral state without any voltage applied. The intensity is very uniform across the drumhead, indicating an undeflected surface. The pixel displays cyan in this state. (ii) corresponds to a top voltage of -5 V and back voltage 0 V. It can be seen the centre area is uniformly deflected and now evinces a purple colour. (iii) corresponds to a top voltage of -5 V and a back voltage of 3 V. The centre of the pixel is further deflected and exhibits a yellow colour. The functional area of the drum is the central region comprising 41% and 31% of the drum area for e(ii) and (iii) states, respectively. This calculation is based on the

colour intensity of the spectra, i.e., the area circled by the dashed lines. Such uniformity should be increased in real applications. This could be achieved by increasing the pixel size, while retaining enough space for the electrical contacts and wires or by pre-patterning of the substrate. After the voltage is removed, the colour of the drum goes back to cyan, as shown in Figure 4 (c). The colour coordinates in the CIE space of the 3 situations are shown in 4 (d). We can see that the colours lie in the cyan, purple and yellow regions, respectively. However, further optimization is needed to capture more of the CIE space.[22] One promising approach is to substitute silicon with materials which have a higher reflectance in the visible range, such as silver or gold.

The current pixel consists of just silicon, silicon dioxide and gold, which are all environmentally friendly materials.[27] The pixel is intrinsically a capacitor with air as the dielectric material. Therefore, the power consumption for different colours is the energy used for charging the capacitor to the corresponding voltages. For the 10-micron pixel discussed here, the energy needed is 32.3 aJ for magenta and 82.6 aJ for yellow, correspondingly. Please refer to Section 3 of the Supporting Information for more details. Moreover, the inert and stable nature of these materials ensures the devices are mechanically robust. In the specific case of our samples, no degradation was noticed after 24 months and countless measurements. The shape of the pixel is only dependent on the shape of the substrate patterns, which is highly controllable. The supporting film showcases two pixels in the shape of the numbers "50" and "51" flashing at a frequency of 25 Hz. Examples of square shaped drum pixels and their colour response under top DC bias and back DC bias are shown in Figure S9 and S10 respectively.

Conclusion

We have developed an interferometric pixel based on a remarkably simple nanoelectromechanical system. The pixel is a Fabry-Pérot cavity constructed from nanometre thick gold

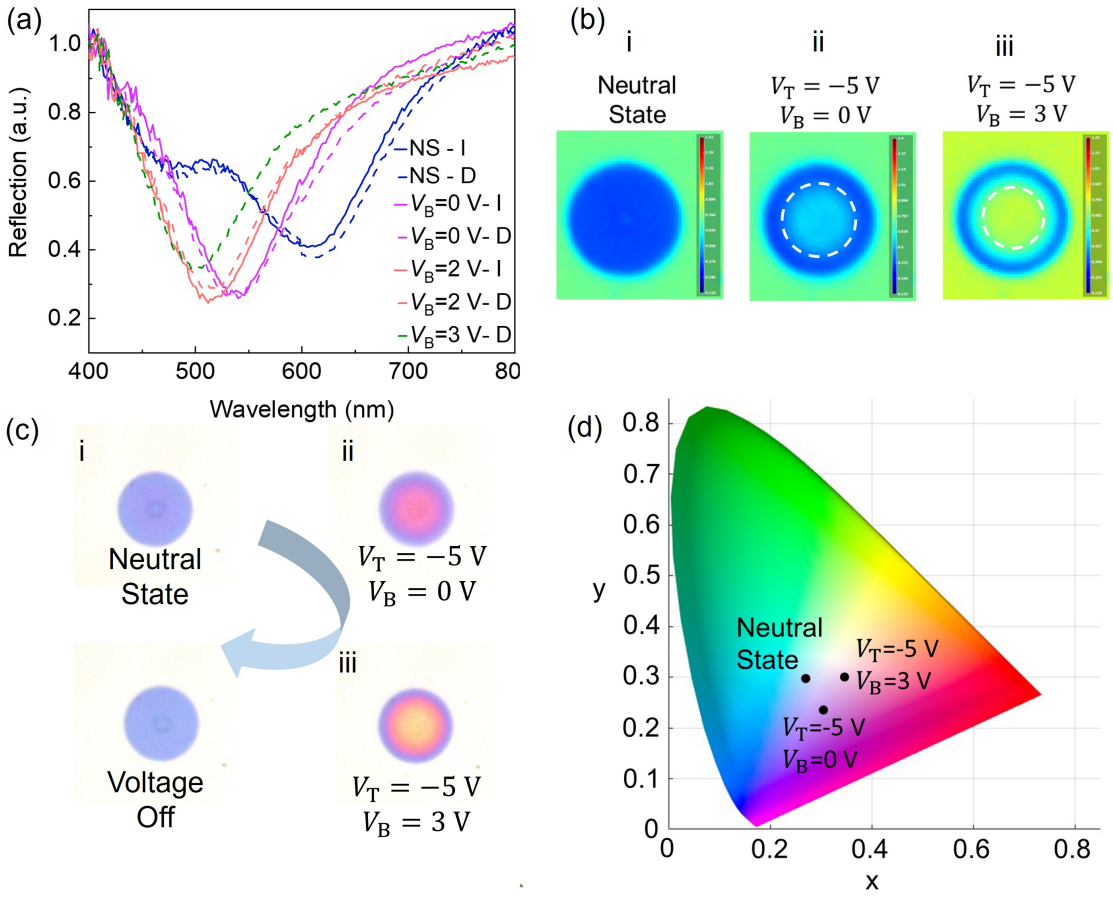


Figure 4: **Spectra of perforated drums.** (a) Reflection spectra taken at the centre of a clean drum and a perforated drum in different situations. NS is short for neutral state. I is short for initial. D is short for defective or perforated. (b) Hyperspectral images of the perforated drum under different driving voltages. (c) Microscope images of the perforated drums under different driving voltages. (d) CIE colour coordinates of the colour displayed at the voltages specified in (b).

films atop a bottom silicon substrate. The intermediate is air and the spacer is silica. The film is deformed when an electric field between the silicon substrate and the film is applied. As the deformation changes, the cavity length changes and thus the colour displayed by the pixel changes. The stable cavity thickness is determined by the equilibrium between the elastic forces and the electrostatic forces acting on the film. The colour cyan, magenta and yellow can be realised under different biases. The pixel also shows good high-frequency response up to MHz levels. The gold nanodrum offers surprisingly diverse though complex colour variations and a novel way to generate reflected colour. Making the pixels into single-pixel addressable arrays is the next step towards application.

Acknowledgement

This work was supported by grants from the ARC (CE170100026, DP160102754, LE210100151), the Department of Industry (ACSRIII00001) and the University of Melbourne Early Career Researcher Grant, Jialu Li, 2023. We appreciate the discussion with Dr. Shi Tang in semiconductor physics. This work was performed in part at the Melbourne Centre for Nanofabrication (MCN) in the Victorian Node of the Australian National Fab- rication Facility (ANFF).

Supporting Information Available

Supporting Information includes Supporting Figures, AC response, power consumption, discussion on experimental and simulation results, fabrication, characterisation and modelling methods, and supporting film.

References

(1) Siegenthaler, E.; Bochud, Y.; Bergamin, P.; Wurtz, P. Reading on LCD vs e-Ink displays: effects on fatigue and visual strain. *Ophthalmic and Physiological Optics* **2012**, *32*, 367–374.

(2) Babu, V. S.; Oliveira, L.; Birrell, S.; Taylor, A.; Cain, R. Comparison of E-ink and OLED screens as train seat displays: a user study. Intelligent Transport Systems–From Research and Development to the Market Uptake: First International Conference, INTSYS 2017, Hyvinkää, Finland, November 29-30, 2017, Proceedings 1. 2018; pp 294–300.

(3) Jin, M.; Shen, S.; Yi, Z.; Zhou, G.; Shui, L. Optofluid-based reflective displays. *Micromachines* **2018**, *9*, 159.

(4) Siegenthaler, E.; Schmid, L.; Wyss, M.; Wurtz, P. LCD vs. E-ink: An Analysis of the Reading Behavior. *Journal of Eye Movement Research* **2012**, *5*, 3.

(5) Daqiqeh Rezaei, S.; Ho, J.; Wang, T.; Ramakrishna, S.; Yang, J. K. Direct color printing with an electron beam. *Nano Letters* **2020**, *20*, 4422–4429.

(6) Daqiqeh Rezaei, S.; Ho, J.; Naderi, A.; Tavakkoli Yaraki, M.; Wang, T.; Dong, Z.; Ramakrishna, S.; Yang, J. K. Tunable, cost-effective, and scalable structural colors for sensing and consumer products. *Advanced Optical Materials* **2019**, *7*, 1900735.

(7) Li, Z.; Butun, S.; Aydin, K. Large-area, lithography-free super absorbers and color filters at visible frequencies using ultrathin metallic films. *Acs Photonics* **2015**, *2*, 183–188.

(8) Kossoy, A.; Merk, V.; Simakov, D.; Leosson, K.; Kéna-Cohen, S.; Maier, S. A. Optical and structural properties of ultra-thin gold films. *Advanced Optical Materials* **2015**, *3*, 71–77.

(9) Yan, M. Metal–insulator–metal light absorber: a continuous structure. *Journal of Optics* **2013**, *15*, 025006.

(10) Shin, H.; Yanik, M. F.; Fan, S.; Zia, R.; Brongersma, M. L. Omnidirectional resonance in a metal–dielectric–metal geometry. *Applied Physics Letters* **2004**, *84*, 4421–4423.

(11) Daqiqeh Rezaei, S.; Dong, Z.; You En Chan, J.; Trisno, J.; Ng, R. J. H.; Ruan, Q.; Qiu, C.-W.; Mortensen, N. A.; Yang, J. K. Nanophotonic structural colors. *ACS Photonics* **2020**, *8*, 18–33.

(12) Streyer, W.; Law, S.; Rooney, G.; Jacobs, T.; Wasserman, D. Strong absorption and selective emission from engineered metals with dielectric coatings. *Optics express* **2013**, *21*, 9113–9122.

(13) Lin, Z.; Long, Y.; Zhu, X.; Dai, P.; Liu, F.; Zheng, M.; Zhou, Y.; Duan, H. Extending the color of ultra-thin gold films to blue region via Fabry-Pérot-Cavity-Resonance-Enhanced reflection. *Optik* **2019**, *178*, 992–998.

(14) Joo, W.-J.; Kyoung, J.; Esfandyarpour, M.; Lee, S.-H.; Koo, H.; Song, S.; Kwon, Y.-N.; Song, S. H.; Bae, J. C.; Jo, A.; others Metasurface-driven OLED displays beyond 10,000 pixels per inch. *Science* **2020**, *370*, 459–463.

(15) Dong, Y.; Akinoglu, E. M.; Zhang, H.; Maasoumi, F.; Zhou, J.; Mulvaney, P. An optically responsive soft etalon based on ultrathin cellulose hydrogels. *Advanced Functional Materials* **2019**, *29*, 1904290.

(16) Miles, M. W. A new reflective FPD technology using interferometric modulation. *Journal of the Society for Information Display* **1997**, *5*, 379–382.

(17) Cartamil-Bueno, S. J.; Davidovikj, D.; Centeno, A.; Zurutuza, A.; van der Zant, H. S.; Steeneken, P. G.; Houri, S. Graphene mechanical pixels for interferometric modulator displays. *Nature communications* **2018**, *9*, 4837.

(18) Zhang, S.; Ren, J.; Chen, S.; Luo, Y.; Bai, X.; Ye, L.; Yang, F.; Cao, Y. Large area electrochromic displays with ultrafast response speed and high contrast using solution-processable and patternable honeycomb-like polyaniline nanostructures. *Journal of Electroanalytical Chemistry* **2020**, *870*, 114248.

(19) Cho, S. I.; Kwon, W. J.; Choi, S.-J.; Kim, P.; Park, S.-A.; Kim, J.; Son, S. J.; Xiao, R.; Kim, S.-H.; Lee, S. B. Nanotube-based ultrafast electrochromic display. *Advanced Materials* **2005**, *17*, 171–175.

(20) Liu, A.; Gao, L.; Zou, W.; Huang, J.; Wu, Q.; Cao, Y.; Chang, Z.; Peng, C.; Zhu, T. High speed surface defects detection of mirrors based on ultrafast single-pixel imaging. *Optics Express* **2022**, *30*, 15037–15048.

(21) Li, J.; Dyer, A.; Smith, D.; Mulvaney, P. Gold Nanodrum Resonators. *ACS nano* **2023**, *17*, 20551–20559.

(22) Manzoor, S. H.; Manzoor, S.; Diez, M. A. P. An Efficient Opto Electronic Filter Design of Reflective CMY Colors for Optical Communications. *Engineering Proceedings* **2023**, *32*, 1.

(23) Schlicke, H.; Battista, D.; Kunze, S.; Schroter, C. J.; Eich, M.; Vossmeyer, T. Free-standing membranes of cross-linked gold nanoparticles: novel functional materials for electrostatic actuators. *ACS applied materials & interfaces* **2015**, *7*, 15123–15128.

(24) Smith, A.; Niklaus, F.; Paussa, A.; Vaziri, S.; Fischer, A. C.; Sterner, M.; Forsberg, F.; Delin, A.; Esseni, D.; Palestri, P.; others Electromechanical piezoresistive sensing in suspended graphene membranes. *Nano letters* **2013**, *13*, 3237–3242.

(25) Erbil, S. O.; Hatipoglu, U.; Yanik, C.; Ghavami, M.; Ari, A. B.; Yuksel, M.; Hanay, M. S. Full electrostatic control of nanomechanical buckling. *Physical review letters* **2020**, *124*, 046101.

(26) Arefev, M. I.; Shugaev, M. V.; Zhigilei, L. V. Kinetics of laser-induced melting of thin gold film: How slow can it get? *Science Advances* **2022**, *8*, eabo2621.

(27) Cao, L.; Fan, P.; Barnard, E. S.; Brown, A. M.; Brongersma, M. L. Tuning the color of silicon nanostructures. *Nano letters* **2010**, *10*, 2649–2654.

TOC Graphic

